

PLGA-PEG-PLGA hydrogel with NEP1-40 promotes the functional recovery of brachial plexus root avulsion in adult rats

Wenlai Guo¹, Bingbing Pei², Zehui Li¹, Xiao Lan Ou¹, Tianwen Sun¹ and Zhe Zhu¹

¹ Department of Hand Surgery, The Second Hospital of Jilin University, Chang chun, Jilin, China

² Department of Orthopedics, Chinese People's Liberation Army Joint Logistics, Support Unit 964 Hospital, Chang chun, Jilin, China

ABSTRACT

Adult brachial plexus root avulsion can cause serious damage to nerve tissue and impair axonal regeneration, making the recovery of nerve function difficult. Nogo-A extracellular peptide residues 1-40 (NEP1-40) promote axonal regeneration by inhibiting the Nogo-66 receptor (NgR1), and poly (D, L-lactide-co-glycolide)-poly (ethylene glycol)-poly (D, L-lactide-co-glycolide) (PLGA-PEG-PLGA) hydrogel can be used to fill in tissue defects and concurrently function to sustain the release of NEP1-40. In this study, we established an adult rat model of brachial plexus nerve root avulsion injury and conducted nerve root replantation. PLGA-PEG-PLGA hydrogel combined with NEP1-40 was used to promote nerve regeneration and functional recovery in this rat model. Our results demonstrated that functional recovery was enhanced, and the survival rate of spinal anterior horn motoneurons was higher in rats that received a combination of PLGA-PEG-PLGA hydrogel and NEP1-40 than in those receiving other treatments. The combined therapy also significantly increased the number of fluorescent retrogradely labeled neurons, muscle fiber diameter, and motor endplate area of the biceps brachii. In conclusion, this study demonstrates that the effects of PLGA-PEG-PLGA hydrogel combined with NEP1-40 are superior to those of other therapies used to treat brachial plexus nerve root avulsion injury. Therefore, future studies should investigate the potential of PLGA-PEG-PLGA hydrogel as a primary treatment for brachial plexus root avulsion.

Submitted 23 March 2021
Accepted 17 September 2021
Published 1 November 2021

Corresponding authors
Tianwen Sun,
suntianwen@jlu.edu.cn
Zhe Zhu, zhuzhe1983@jlu.edu.cn

Academic editor
Vladimir Uversky

Additional Information and
Declarations can be found on
page 13

DOI 10.7717/peerj.12269

© Copyright
2021 Guo et al.

Distributed under
Creative Commons CC-BY 4.0

OPEN ACCESS

Subjects Biochemistry, Neuroscience, Neurology, Histology

Keywords PLGA-PEG-PLGA, Brachial plexus avulsion, NEP1-40, Nerve regeneration

INTRODUCTION

Brachial plexus avulsion (BPA) is a commonly observed injury in young adults and is often caused by severe trauma, such as that associated with car accidents (*Faglioni et al., 2014*). After BPA, the nerve root is torn from the spinal cord, which causes loss of sensory and motor functions in the corresponding area of innervation. The initial insult and secondary damage result in widespread neuronal death. Unfortunately, nerve regeneration is difficult because of various inhibitory factors, and recovery is almost impossible without surgical treatment. Further, simple surgical treatment often leads to unsatisfactory

results that are accompanied by a high disability rate ([Carlstedt, 2008](#); [Gibon et al., 2016](#); [Lang et al., 2005](#)).

Replantation of the avulsed nerve root *in situ* is the ideal treatment for BPA. Replantation can not only restore the anatomical structure and avoid injuries caused by other reconstructive interventions ([Eggers et al., 2010](#); [Limthongthang et al., 2013](#); [Shin et al., 2005](#)), but also greatly reduces post-injury neuralgia ([Ciaramitaro et al., 2017](#); [Teixeira et al., 2015](#); [Zhou et al., 2017](#)). Nevertheless, various inhibitory factors produced in post-injury nerve tissue, limit neural regeneration and result in poor functional recovery ([So & Xu, 2015](#)). To promote the recovery of nerve function, more attention has been given to the promotion of axon regeneration or the elimination of inhibitory factors associated with nerve damage.

Nogo receptors (NgRs), including NgR1, NgR2, and NgR3, are endogenous myelin-associated protein-related receptors in the central and peripheral nerves ([Chen et al., 2000](#); [Young, 1996](#)). Nogo-A, the ligand with the highest affinity for NgR1, can bind to NgR1, inhibit axonal growth, resulting in growth cone collapse. Nogo-A extracellular peptide residues 1-40 (NEP1-40), the most common NgR1 antagonist, comprises a small polypeptide that competes with NgR1 by targeting Nogo-66, the main inhibitory region of Nogo-A ([GrandPré, Li & Strittmatter, 2002](#)). Therefore, NEP1-40 can relieve the neurosuppressive effect of Nogo-A ([Cao et al., 2008](#); [Chen et al., 2000](#); [GrandPré, Li & Strittmatter, 2002](#); [Kempf & Schwab, 2013](#); [Xu et al., 2017](#)), increase the expression of growth-associated protein 43 (GAP-43) and microtubule-associated protein 2 (MAP-2) in nerve tissue, reduce the levels of amyloid- β (A β) precursor protein (APP), and, consequently, facilitate nerve regeneration, axonal growth as well as functional recovery ([Li & Strittmatter, 2003](#); [Mingorance et al., 2006](#); [Wang et al., 2007](#); [Xu et al., 2017](#)).

BPA can (i) cause nerve tissue defects, lead to an irregular cavity at the junction area between the spinal cord and the brachial plexus, (ii) subsequently inducing the excessive build-up of scar tissue, and, (iii) finally, impact the penetration of axons ([Carlstedt, 2008](#); [Meng et al., 2019, 2020](#)). Therefore, the use of appropriate filling materials with a drug load may be employed to promote nerve regeneration ([Baazil et al., 2015](#); [Ding et al., 2019](#)). Poly (D, L-lactide-co-glycolide)-poly (ethylene glycol)-poly (D, L-lactide-co-glycolide) (PLGA-PEG-PLGA) is a temperature-sensitive hydrogel that has a wide range of applications in drug delivery owing to its good biocompatibility and safety. The fluidity and gel-forming properties of PLGA-PEG-PLGA allow it to effectively fill in tissue defects and sustain the delivery of drugs to the site of injury ([Ding et al., 2019](#); [Zhang et al., 2014](#)). Further, studies have reported that combinations of PLGA-PEG-PLGA hydrogel with drugs can be more efficacious than drugs alone ([Ding et al., 2019](#); [Huang et al., 2020](#)). Because treatment with drugs alone, if it is intravenous injection, after the metabolism of the various organs of the body, the actual dose of the drug reaching the injured site is very small, and it cannot even meet the needs of the injured site for treatment. Simply increasing the injected dose will not only affect the function of the other organs, and more drugs are wasted. If the drug is injected directly *in situ*, the fluidity of the drug liquid and the irregular shape of the injured site will cause the loss of most drugs and the utilization rate is low. But the drug-loaded hydrogel can provide excellent encapsulation

for NEP1-40 and avoid sudden release of it. Therefore, it will increase the efficacy of the drug (Macaya & Spector, 2012; Shrestha et al., 2014; Zhang et al., 2011). Therefore, it can facilitate nerve regeneration. The current study aimed to examine the effects of PLGA-PEG-PLGA hydrogel loaded with NEP1-40 on neural regeneration in an adult rat model of BPA and evaluate the mechanisms underlying regeneration.

MATERIALS & METHODS

Materials

PEG (Mn = 1,500 g/mol), D, L-Lactide (D, L-LA), glycolide (GA), Tin (II) 2-ethylhexanoate (Sn(Oct)₂), methyl thiazolyl tetrazolium, and quercetin were purchased from Sigma–Aldrich (Sigma, St Louis, MO, USA). NEP1-40 was purchased from TOCRIS (Bristol, UK). Sheep anti-rat choline acetyltransferase (ChAT) antibody was purchased from Millipore (Darmstadt, Germany), while rabbit anti-goat fluorescence 568 antibody and alpha-bungarotoxin (α-BTX) 594 antibody were purchased from Abcam (Cambridge, UK) and Invitrogen (Waltham, MA, USA), respectively. Fluoro-Gold (FG) was purchased from Fluorochrome, LLC. (Denver, CO, USA). All chemical reagents were used directly without further purification.

Synthesis of the temperature-sensitive PLGA-PEG-PLGA hydrogel

As described previously (Ci et al., 2014; Zhao, Guo & Ma, 2014), firstly, 68 g of PEG, 115 g of D, L-LA, and 35 g of GA were dehydrated by vacuum drying for 48 h. Subsequently, 30 mg of Sn (Oct)₂ was added as a catalyst at 120 °C, and the reaction was allowed to continue for 48 h. The reaction product was sufficiently dissolved in 500 mL cold water at 4 °C, and the solution was heated to 80 °C for precipitation and purification. The purification process was repeated thrice, and the purified product was dried in a vacuum for later use.

Characterization of PLGA-PEG-PLGA

Experimental data were recorded using a Bruker DMX500 spectrometer (Switzerland) at 500 MHz Deuterated chloroform (CDCl₃) was used as a solvent, and tetramethylsilane was used as an internal standard. The sol–gel transition temperature of the PLGA-PEG-PLGA triblock copolymer was determined by the vial inversion test. Different quantities of PLGA-PEG-PLGA polymer were dissolved in phosphate-buffered saline (PBS), and the vial containing 0.5 mL of the polymer solution was stored for 15 min prior to the measurement. The temperature increment was set at 1 °C. The gel was successfully formed when the solution in the vial did not flow after being inverted for 30 s.

Release profiles of NEP1-40 from PLGA-PEG-PLGA hydrogels

As described above, the optimal mass concentration of the PLGA-PEG-PLGA polymer was prepared. Then, NEP1-40 was dissolved in acetone and added to the PLGA-PEG-PLGA solution. Subsequently, the PLGA-PEG-PLGA polymer loaded with NEP1-40 was added to a test tube with an inner diameter of 16 mm and incubated at 37 °C for 10 min. After the hydrogels were formed, 5 mL of PBS were added to the top of the gels, and

the test tubes were placed at 37 °C with continuous shaking at 60 rpm. Subsequently, 1 mL of PBS was regularly aspirated and replenished every 2 days, with a total time of 14 days (Nakamura *et al.*, 2011; Xu *et al.*, 2017; Zhai & Feng, 2019). The amount of NEP1-40 in the aspirated PBS extract was measured using an ultraviolet spectrophotometer at 306 nm, and drug release profile was constructed on the basis of the obtained absorbance values.

Experimental animals and groups

Animal procedures were conducted in accordance with the guidelines for the review and approval of the Animal Care and Use Committee of Jilin University (Ethical Approval No. 2018-119), and followed the Guide for the Care and Use of Laboratory Animals issued by the USA National Institutes of Health (National & Promising, 2009). Effort was made to minimize pain and the number of animals used in the experiments. The dose used for anesthesia is 45 mg/kg of 3% pentobarbital sodium (New Asia Pharmaceutical, Shanghai, China), and the dose used for euthanasia is 200 mg/kg of 3% pentobarbital sodium.

Forty healthy female adult Sprague–Dawley rats (weight, 200–250 g; age, 10–12 weeks) were provided by the Animal Experimental Center of Jilin University in China. The reasons why we choose female adult rats are as following: (1) female rats are less aggressive and have no sense of territory, so they are less aggressive to each other; while male rats have territorial awareness, they may attack each other, causing the experiment to fail; (2) after brachial plexus injury, some rats will be aggressive or eat limbs that do not feel sensation due to loss of sensation on one side. Females are less aggressive, so they are less likely to eat their limbs. All animals were caged in standard animal rooms at 22 °C with free access to food and water. The rats were randomized into the following four groups ($n = 10$ /group): control group, blank hydrogel group, NEP1-40 group, and NEP1-40-loaded hydrogel group. Experienced technicians for health and behavior monitored the animals daily during the protocol. The animals were weighed weekly. No rats displayed markers associated with death or poor prognosis of quality of life, or specific signs of severe suffering or distress, which would have led to early and immediate euthanasia.

Model preparation and treatments

The rats were intraperitoneally anesthetized using 45 mg/kg of 3% pentobarbital sodium. The BPA model was established according to the methods described by Gu *et al.* (2004). Briefly, the backs of rats were depilated, and the lamina and spinous processes from the fourth cervical spine (C4) to the second thoracic spine (T2) were exposed *via* the dorsal approach. The dorsal lamina of the right C5–C7 was opened followed by exposure and avulsion of the C5–C7 nerve roots. The C5 and C7 nerve roots (about 5 mm in length) were excised, and the distal ends of the nerve roots were retracted to prevent regeneration. The C6 nerve root was replanted to the spinal cord, and the muscles and skin were sutured after hemostasis. After surgery, the animals were maintained in a clean environment and administered an intramuscular injection of cefazolin sodium (50 mg/kg,

Table 1 Grouping and treatments.

| | Control group | Blank hydrogel group | NEP1-40 group | NEP1-40-loaded hydrogel group |
|--|---------------|----------------------|-----------------|---|
| Material loaded around the replanted C6 nerve root | (–) | 100 µL hydrogel | (–) | 100 µL, 0.5 mg/mL NEP1-40—loaded hydrogel |
| Intraperitoneal injection | PBS/DMSO | PBS/DMSO | 12.5 µg NEP1-40 | PBS/DMSO |

twice a day; Zhong-nuo Pharmaceutical) as anti-infection treatment for 3 consecutive days (Birrell & Fuller, 2019; Kusaba, 2009).

In the control group, the surgical incision was sutured directly, and a 100 µL mixture of PBS and dimethyl sulfoxide (DMSO) (83% PBS + 17% DMSO) was administered intraperitoneally once a day for 14 consecutive days (Table 1). In the blank hydrogel group, 100 µL of hydrogel was injected around the replanted C6 nerve root and held for 3 min. The incision was sutured until the hydrogel was stabilized. Postoperatively, a 100 µL mixture of PBS and DMSO (83% PBS + 17% DMSO) was intraperitoneally administered once a day for 14 consecutive days (Table 1). In the NEP1-40 group, the surgical incision was directly sutured, and 12.5 µg of NEP1-40 were dissolved in a 100 µL mixture of PBS and DMSO (83% PBS + 17% DMSO) and intraperitoneally injected once a day for 14 consecutive days (Table 1) (Nakamura *et al.*, 2011; Steward *et al.*, 2008; Xu *et al.*, 2017). In the NEP1-40-loaded hydrogel group, 100 µL of 0.5 mg/mL NEP1-40-loaded hydrogel was injected around the replanted C6 nerve root and allowed to stabilize for 3 min. The incision was then sutured. Postoperatively, a 100 µL mixture of PBS and DMSO (83% PBS + 17% DMSO) was intraperitoneally administered once a day for 14 consecutive days (Table 1).

Behavioural test

Between weeks 2 and 6 post-surgery, eight rats from each group were subjected to the Terzis grooming test (TGT) test to evaluate motor function of the affected upper limb (Bertelli & Mira, 1993; So & Xu, 2015). Two investigators who did not participate in model induction graded the motor function of the right upper limb. Divergences between assessments of the two investigators were independently resolved by a third investigator.

Immunofluorescence assay and FG nerve retrograde labeling

At 6 weeks post operation, three rats from each group were randomly selected and sacrificed. After infusion with 4% paraformaldehyde, the spinal C6 segment was dissected and cut into 25-µm thick sections. One out of every four sections was incubated with the anti-ChAT (1:100; Millipore) antibody at 4 °C overnight. The following day, sections were incubated with the secondary antibody at 18–22 °C for 1.5 h (Alexa Fluor[®] 568 rabbit anti-goat IgG; Abcam). ChAT-positive spinal anterior horn motoneurons on the injured side and contralateral side were counted under a fluorescence microscope to assess the cell ratio of the injured side to the healthy side.

At 6 weeks post operation, three rats were randomly selected from each group. They were anesthetized and a transverse incision was made below the right clavicle. The pectoralis major and minor muscles were cut off to expose and dissociate the

musculocutaneous nerve of the right side. A glass needle was inserted 5 mm proximal to the nerve entry point of the musculocutaneous nerve into the biceps muscle, and 0.8 μ L of FG was carefully injected into the musculocutaneous nerve with a microinjection pump. The needle was retained for 10 s until the FG was completely absorbed. The muscle and skin were sutured layer by layer. Postoperative anti-infection treatment was administered for 3 consecutive days. Subsequently, the rats were subjected to cardiac perfusion using 4% paraformaldehyde, and the C5–C8 segments were longitudinally cut into 25- μ m thick sections. One out of every four sections was observed under a fluorescence microscope to assess the number of FG-labeled neurons.

Immunofluorescence detection of muscle fiber diameter in the injured biceps and assessment of the amount and morphology of motor endplate (MEP) neurons in the injured biceps muscle by immunofluorescence

At 6 weeks post operation, four rats were randomly selected and sacrificed from each group and subjected to cardiac perfusion using 4% paraformaldehyde. The biceps muscles on the injured side were dissected, cut into 14- μ m thick sections, and stained with hematoxylin-eosin. We randomly selected and photographed 50–100 muscle fibers from each biceps muscle under a light microscope. Image-J (National Institutes of Health, Bethesda, MD, USA) was used to measure the diameter of the muscle fiber, and the average value was calculated.

One out of every four sections was used to stain the MEP. The sections were incubated with α -BTX 594 antibody in 0.01 M PBS (α -BTX 594: 0.01M PBS = 1:400) for 30 min, and the morphology of the MEPs was observed under a microscope. At least 150 MEPs were randomly selected from each animal specimen and photographed. Image-J analysis software was used to measure the area of the MEPs.

Statistical analyses

Graph-Pad Prism 5.0 cartography software (Graph-Pad Software, Inc., CA, USA) was used for mapping, and SPSS 15.0 software (SPSS, Chicago, IL, USA) was used for one-way analysis of variance. Measurement data are expressed as means \pm standard deviation (SD). A pairwise comparison was performed using the Students *t*-test. Differences with a *P*-value of ≤ 0.05 were considered statistically significant.

RESULTS AND DISCUSSION

Material characterization and release profile of NEP1-40

PLGA-PEG-PLGA temperature-sensitive hydrogel can (i) fill defected tissues, (ii) restrict the ingrowth of some cell types, including fibroblasts and inflammatory cells, and (iii) prevent astrocyte proliferation, thereby minimizing the formation of scar tissue. New tissues will completely fill the injured area following the absorbance, degradation, and disappearance of the scaffold (Luo, Borgens & Shi, 2004; Rong et al., 2019; Zhang et al., 2014). In this study, we first synthesized PLGA-PEG-PLGA hydrogels and determined their properties.

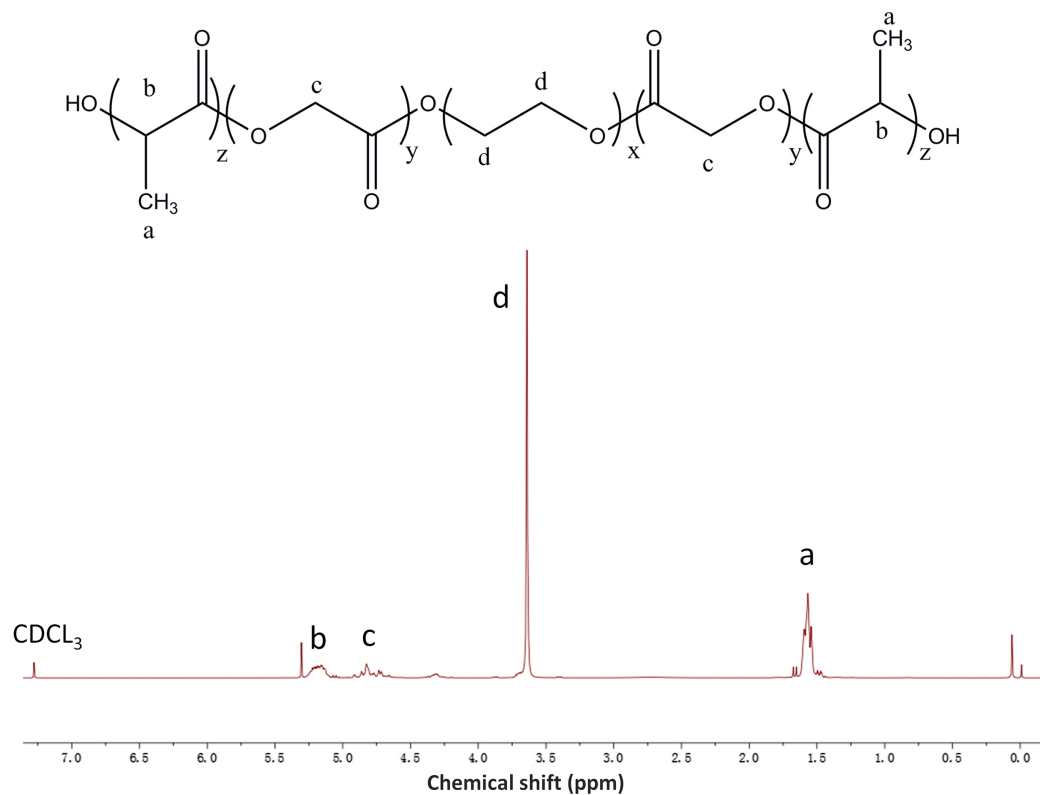


Figure 1 The ^1H NMR spectrum of the PLGA-PEG-PLGA copolymer in CDCl_3 . The characteristic signals appearing at 5.2, 4.8, 3.5, and 1.5 ppm represent the CH of LA, CH_2 of GA, CH_2 of PEG, and CH_3 of LA, respectively. [Full-size !\[\]\(fd7fe780e8fd8eece60268c87d0c3e04_img.jpg\) DOI: 10.7717/peerj.12269/fig-1](https://doi.org/10.7717/peerj.12269/fig-1)

The composition and structure of the PLGA-PEG-PLGA copolymer were determined using ^1H NMR spectroscopy (Fig. 1). We observed a complicated split in these peaks owing to the random copolymerization of GA and LA, and the characteristic signals that appeared at 5.2, 4.8, 3.5, and 1.5 ppm represented the CH of LA, CH_2 of GA, CH_2 of PEG, and CH_3 of LA, respectively. Studies have revealed that there is a close association between the sol-gel transition of PLGA-PEG-PLGA hydrogel and its concentration (Zhang *et al.*, 2011). In this study, the vial inversion test was performed to explore the sol-gel transition of the hydrogels (Fig. 2), and a typical sol-gel-precipitation transition was observed when the hydrogel concentration was 15–30%. Our findings revealed that a higher PLGA-PEG-PLGA concentration was associated with a higher gel-precipitation transition temperature and a lower sol-gel transition temperature, and a 30 wt% PLGA-PEG-PLGA hydrogel had a wider gel window. Therefore, the 30 wt% PLGA-PEG-PLGA hydrogel was selected for later use because of its appropriate sol-gel transition temperature.

We measured and plotted the drug release profile (Fig. 3) to observe the release of NEP1-40 from the PLGA-PEG-PLGA hydrogel. A rapid release of about 37% NEP1-40 was observed on day 1, and about 70% of NEP1-40 had been released within 14 days in a relatively smooth sustained-release trend. These findings indicate that the hydrogel can sustain drug release for at least 14 days.

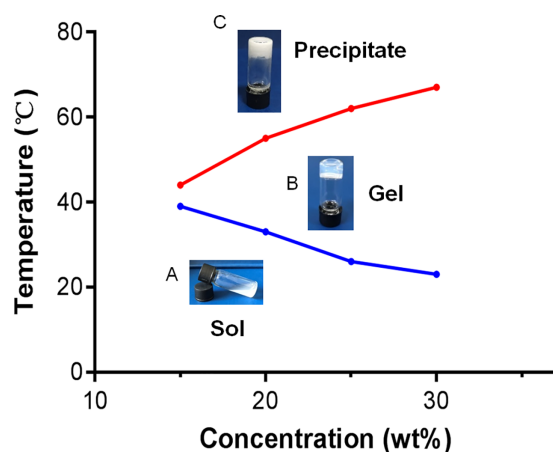


Figure 2 Sol-to-gel transition temperature measurement of PLGA-PEG-PLGA copolymers determined using the vial inversion test and phase diagram of the sol-gel-precipitation transition as a function of PLGA-PEG-PLGA concentration. (A) Copolymers in the sol state; (B) Copolymers in the gel state; (C) Copolymers in the precipitate state. PLGA-PEG-PLGA: poly (D, L-lactide-co-glycolide)-poly (ethylene glycol)-poly (D,L-lactide-co-glycolide).

Full-size DOI: 10.7717/peerj.12269/fig-2

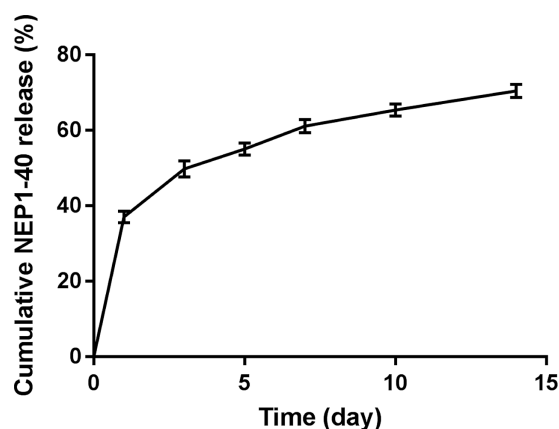


Figure 3 Cumulative release profile of NEPI-40. On day 1, about 37% NEPI-40 was released from the PLGA-PEG-PLGA hydrogel. During days 2–14, 70% of the NEPI-40 was steadily released. Data are presented as means \pm standard errors ($n = 3$).

Full-size DOI: 10.7717/peerj.12269/fig-3

Treatment with the NEPI-40-loaded hydrogel sustained-release system significantly improves the function of biceps brachii on the injured side after nerve root replantation for BPA

Steward et al. (2008) showed that early application of NEPI-40 for 14 days can promote the recovery of spinal cord injury. And considering that the recovery period of brachial plexus injury (6–8 weeks) is shorter than that of spinal cord injury, and the time required for spinal cord axons to cross the spinal cord-peripheral nerve junction is shorter than that of spinal cord injury, therefore, we consider 14 days as the appropriate treatment time in our experiment (*Nakamura et al., 2011; Xu et al., 2017; Zhai & Feng, 2019*).

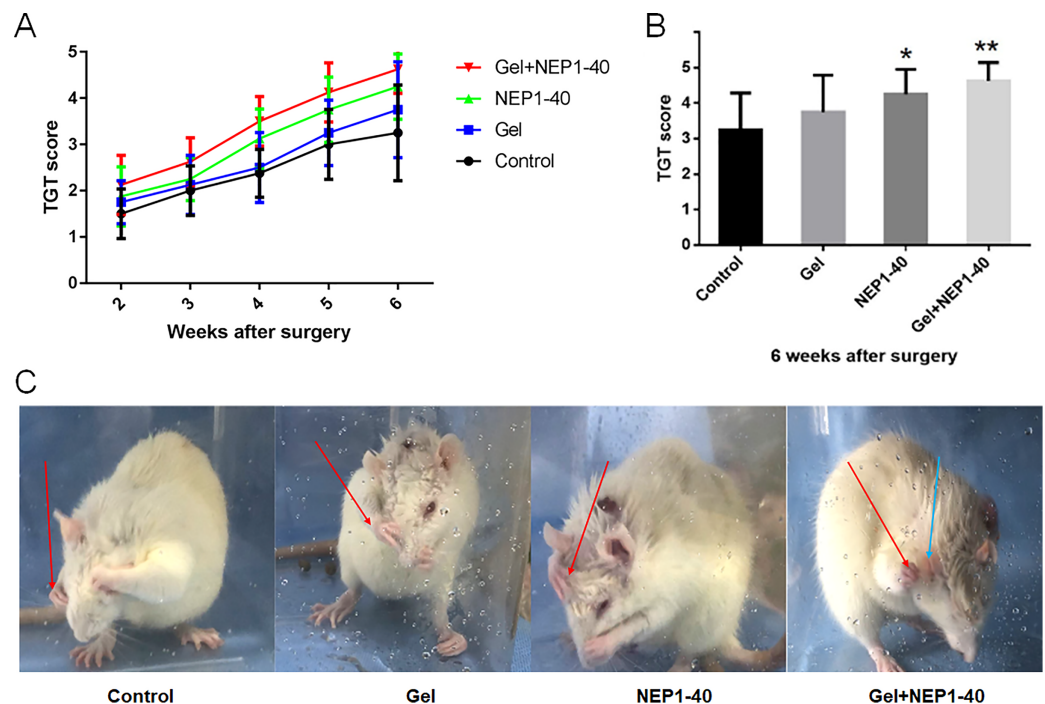


Figure 4 TGT scores ($n = 8$) of the control, blank hydrogel, NEP1-40, and NEP1-40-loaded hydrogel groups at 2–6 weeks post-surgery. (A) TGT scores in each group at 2–6 weeks post-surgery. (B) TGT scores in each group at 6 weeks post-surgery (* $P < 0.05$, ** $P < 0.01$). (C) Representative images of the rats at 6 weeks post-surgery. The rat in the control group did not touch its eyes with the affected upper limb (right), but the rat in the Gel+NEP1-40 group reached the ears with the affected upper limb (right). Arrow red: right upper limb; arrow blue: ear. [Full-size !\[\]\(43e4e85f3e07c993849f98a1fa87e486_img.jpg\) DOI: 10.7717/peerj.12269/fig-4](https://doi.org/10.7717/peerj.12269/fig-4)

BPA model is confirmed by TGT as all the affected upper limb of animals found to receive grade of 0 on postoperative days 1 and 2 (Bertelli & Mira, 1993). This suggested that we successfully established the BPA model. Recovery of nerve function was the most important goal of our study. First, we investigated whether the NEP1-40 hydrogel sustained-release treatment improved the recovery of motor function in rats. We found that the NEP1-40 hydrogel sustained-release system promoted motor function of the upper limbs after nerve root replantation for BPA. At 2–6 weeks after injury, TGT scores were higher in the NEP1-40-loaded hydrogel group than those in the control, blank hydrogel, and NEP1-40 groups. At 2–3 weeks after injury, TGT scores were significantly higher in the NEP1-40-loaded hydrogel group than those in the other groups, indicating a rapid recovery of nerve function. At 4 weeks after injury, TGT scores were rapidly increased in the four groups, and this increase was faster in the NEP1-40 and the NEP1-40-loaded hydrogel groups than in the other groups (Fig. 4A). At 6 weeks post-surgery, the average TGT scores were 3.25, 3.75, 4.25, and 4.63 in the control, blank hydrogel, NEP1-40, and NEP1-40-loaded hydrogel groups, respectively (Figs. 4B and 4C). TGT scores were significantly higher in the NEP1-40 (Fig. 4B; * $P < 0.05$) and NEP1-40-loaded hydrogel group (Fig. 4B; ** $P < 0.01$) than in the control group. TGT scores in the blank hydrogel group were also higher than those in the control group, but this difference was not obvious. Therefore, treatment with the NEP1-40-loaded hydrogel

sustained-release system significantly increased the TGT scores of the affected limbs, indicating that nerve function recovered well (*GrandPré, Li & Strittmatter, 2002*).

Treatment with the NEPI-40-loaded hydrogel sustained-release system significantly increases the survival rate of anterior horn motoneurons and the number of functional motoneurons on the injured side

Neuronal survival is the basis of nerve regeneration. In this study, we observed the number of anterior horn motoneurons and functional motoneurons in the injured spinal cord. The spinal anterior horn motoneurons labeled by ChAT, a specific antibody which can help to distinguish between neuron and other tissues, were significantly bigger (their morphology was similar to normal) in the NEPI-40-loaded hydrogel group than in the other groups at 6 weeks post-surgery. Therefore, neuronal function was better preserved in the NEPI-40-loaded hydrogel group than in the remaining groups. The cell number ratios between the injured and healthy sides were 51.33%, 57.33%, 72.33%, and 75.67% (*Fig. 5E*; $*P < 0.05$). Ratios were higher in the NEPI-40 and NEPI-40-loaded hydrogel groups than in the control group (*Fig. 5E*; $*P < 0.05$).

FG nerve retrograde labeling of the C5–C8 segments revealed that the number of motoneurons in the spinal cord and their size increased significantly after treatment with the NEPI-40-loaded hydrogel sustained-release system (*Figs. 5F–5J*; $*P < 0.05$, $**P < 0.01$), indicating that the number of neurons involved in motor function was increased.

Due to the fact that the anterior horn motor neurons are limited to the anterior horn of the spinal cord, so the range is small. There are no positive cells in other places, which are blank. So, in order to display the cells more intuitively, parts with obvious cells are only put there (the original figures could be seen in the [Supplemental File](#)). Furthermore, the number of functional motoneurons was higher in the NEPI-40 treatment group than in the control treatment group (*Fig. 5J*; $*P < 0.05$). The number of functional motoneurons was slightly but insignificantly increased in the blank hydrogel group as compared to the control group.

Regenerated axons need to pass through or bypass scar tissue in the injured area. Scar tissues contain various nerve growth inhibitory factors that make axonal regeneration tortuous and increase the probability of neural mismatch. Thus, the efficiency of axonal regeneration is decreased, and the difficulty of nerve regeneration is increased (*Cullheim, Carlstedt & Risling, 1999*; *Soderblom et al., 2013*). After BPA, nerve root replantation initiates axon regeneration and increases the survival rate of numerous neurons (*Gu et al., 2004*). Furthermore, axons grow rapidly, and the survival rate of neurons is greatly improved (*Li et al., 2015*). Our results revealed that NEPI-40 promoted axonal growth, thereby preventing necrosis of neurons. Therefore, NEPI-40 had a certain neuroprotective effect, providing a good foundation for nerve regeneration. In addition, we assessed the number of functional motoneurons: the number of FG-labeled neurons was significantly higher after treatment with the NEPI-40-loaded hydrogel sustained-release system than after control treatment (the control group) (*Fig. 5J*; $**P < 0.01$) or the NEPI-40-alone treatment (the NEPI-40 group) (*Fig. 5J*, $*P < 0.05$). This finding indicates that hydrogel

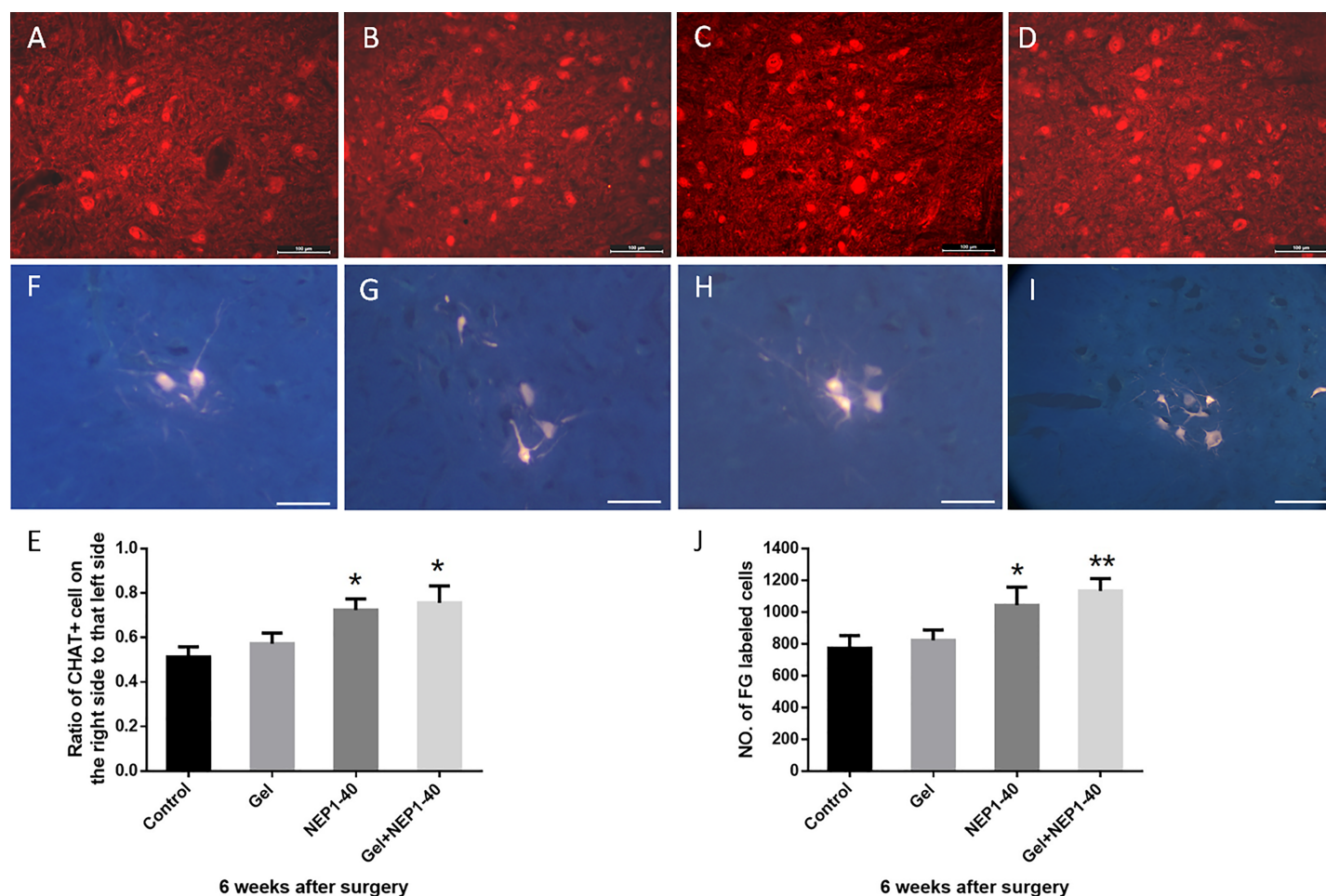


Figure 5 Survival rates of anterior horn motoneurons and the number of FG-labeled motoneurons on the injured side C6 segment at 6 weeks post-surgery. (A–D) ChAT (+) neurons (red) of the C6 spinal segment in the control (A), blank hydrogel (B), NEPI-40 (C), and NEPI-40-loaded hydrogel (D) groups, respectively (scale bar = 100 μ m). (E) Survival rates of anterior horn motoneurons of the C6 segment ($n = 3$, $*P < 0.05$). (F–I) FG nerve retrograde labeling of anterior horn motoneurons of the C5–C8 segments in the control (F), blank hydrogel (G), NEPI-40 (H), and NEPI-40-loaded hydrogel (I) groups, respectively ($n = 3$, scale bar = 100 μ m). (J) The number of FG-labeled anterior horn motoneurons of the C5–C8 segments ($n = 3$, $*P < 0.05$, $**P < 0.01$). [Full-size !\[\]\(e4c51d9db35ee9651ed60d72acdb782c_img.jpg\) DOI: 10.7717/peerj.12269/fig-5](https://doi.org/10.7717/peerj.12269/fig-5)

and NEPI-40 treatment have synergistic effects, and more neurons participate in functional recovery, thereby promoting the restoration of nerve function.

Treatment with the NEPI-40-loaded hydrogel sustained-release system can promote the regeneration of bicep muscle fibers and MEPs on the injured side

After BPA, denervation of muscle tissues leads to atrophy and dysfunction (Duijnsveld *et al.*, 2017). Regeneration and growth of axons into target muscles allows for the recovery of atrophic muscles, fibrosis reversion of muscle fibers, and thickening of the diameter of muscle fibers to adapt to functional changes. MEPs in the muscles are concurrently re-innervated, and the MEP size is enlarged, recovering the original structure (Ali *et al.*, 2016).

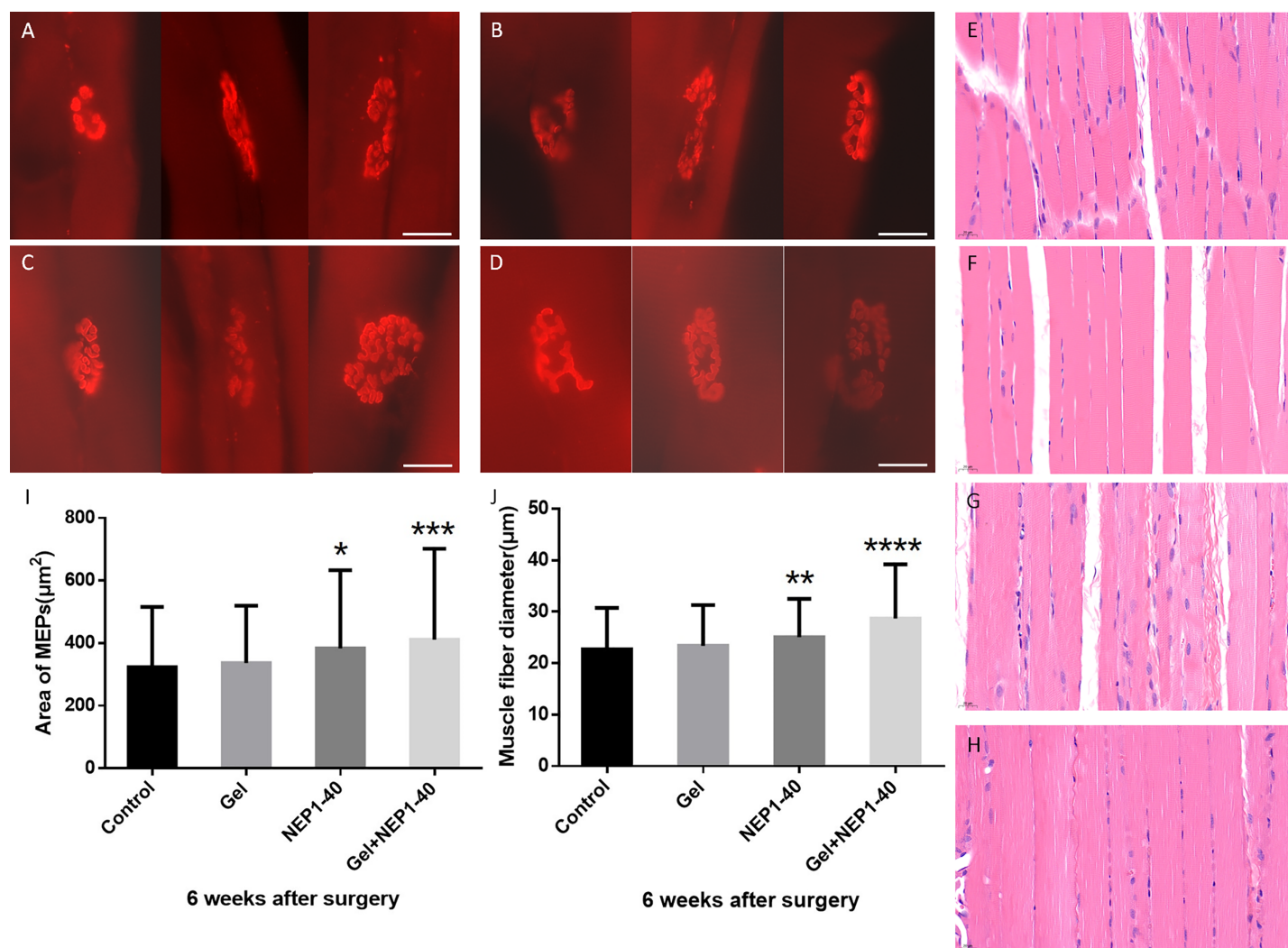


Figure 6 Immunofluorescence staining of MEPs of the injured biceps brachii and hematoxylin-eosin staining of muscle fibers in the control (A), blank hydrogel (B), NEP1-40 (C), and NEP1-40-loaded hydrogel groups (D) at 6 weeks post-surgery. A–D: MEPs of the injured biceps brachii in each group (red) ($n = 4$, scale bar = 20 μm). E–H: Hematoxylin-eosin staining of the biceps brachii in the control (E), blank hydrogel (F), NEP1-40 (G), and NEP1-40-loaded hydrogel (H) groups, respectively ($n = 4$, scale bar = 20 μm). (I) The area of MEPs of the biceps brachii on the injured side at 6 weeks post-surgery (* $P < 0.05$, ** $P < 0.01$). (J) Muscle fiber diameter of the biceps brachii on the injured side at 6 weeks post-surgery (** $P < 0.01$, **** $P < 0.0001$). Full-size DOI: 10.7717/peerj.12269/fig-6

MEPs can be an important indicator of muscle function recovery after reinnervation (Wang et al., 2018). Measurements of the area of motor endplates in the injured biceps brachii at 6 weeks post-surgery revealed that MEP area increased more significantly after treatment with the NEP1-40-loaded hydrogel sustained-release system than with the other treatments (other groups). Additionally, MEP structure was clearer and more complex after treatment with the NEP1-40-loaded hydrogel sustained-release system than after other treatments. The area of MEPs in the NEP1-40-loaded hydrogel group was 27.3% higher than in the control group (Figs. 6A–6D, and 6I; ** $P < 0.01$), indicating that the NEP1-40-loaded hydrogel sustained-release system provides an anatomical basis for functional recovery. The size and complexity of MEPs were higher, and the area of MEPs

was 18.7% higher in the NEP1-40 treatment group than in the control group (Figs. 6A–6D, and 6I; $*P < 0.05$), indicative of the effectiveness of NEP1-40 treatment.

Regenerated axons enter MEPs to trigger an increase in the volume of target muscle fibers, thereby leading to functional recovery. We performed hematoxylin-eosin staining of the muscle fibers of the injured biceps brachii at 6 weeks post-surgery and assessed fiber diameter. We found that muscle fiber diameter was the highest in the NEP1-40-loaded hydrogel group. Additionally, the muscle fiber diameter was 28.8% higher in the NEP1-40-loaded hydrogel group and 16% higher in the NEP1-40 group than in the control group (Figs. 6E–6H, and 6J; $****P < 0.0001$, $**P < 0.01$, respectively). The increase in muscle fiber diameter indicates a good recovery of function. However, muscle fiber diameter in the blank hydrogel group was only slightly higher than in the control group.

CONCLUSION

Our findings indicate that the sustained release of NEP1-40 from the PLGA-PEG-PLGA hydrogel promotes nerve regeneration and recovery of motor function in BPA rats, promotes axonal growth, and protects neurons. The PLGA-PEG-PLGA hydrogel acts as a slow-release carrier and concurrently fills defects, thereby providing favorable conditions for nerve regeneration. Therefore, the combination of NEP1-40 and PLGA-PEG-PLGA hydrogel can promote axonal growth and recovery of nerve function. The present findings shed light on the potential application of the PLGA-PEG-PLGA hydrogel for the treatment of brachial plexus root avulsion.

ADDITIONAL INFORMATION AND DECLARATIONS

Funding

This study was supported by the Jilin Provincial Educational 135 Science and Technology Project (JJKH20190047KJ). The funders had no role in study design, data collection and analysis, decision to publish, or preparation of the manuscript.

Grant Disclosures

The following grant information was disclosed by the authors:

Jilin Provincial Educational 135 Science and Technology Project: JJKH20190047KJ.

Competing Interests

The authors declare that they have no competing interests.

Author Contributions

- Wenlai Guo conceived and designed the experiments, analyzed the data, prepared figures and/or tables, authored or reviewed drafts of the paper, and approved the final draft.
- Bingbing Pei performed the experiments, prepared figures and/or tables, and approved the final draft.
- Zehui Li performed the experiments, authored or reviewed drafts of the paper, and approved the final draft.

- Xiao Lan Ou performed the experiments, prepared figures and/or tables, and approved the final draft.
- Tianwen Sun performed the experiments, analyzed the data, authored or reviewed drafts of the paper, and approved the final draft.
- Zhe Zhu conceived and designed the experiments, performed the experiments, prepared figures and/or tables, authored or reviewed drafts of the paper, and approved the final draft.

Animal Ethics

The following information was supplied relating to ethical approvals (*i.e.*, approving body and any reference numbers):

This study was approved by the Research Ethics Committee of the Second Hospital of Jilin University (Ethical Approval No. 2018-119).

Data Availability

The following information was supplied regarding data availability:

The raw measurements are available in the [Supplemental File](#).

Supplemental Information

Supplemental information for this article can be found online at <http://dx.doi.org/10.7717/peerj.12269#supplemental-information>.

REFERENCES

- Ali ZS, Johnson VE, Stewart W, Zager EL, Xiao R, Heuer GG, Weber MT, Mallela AN, Smith DH. 2016.** Neuropathological characteristics of brachial plexus avulsion injury with and without concomitant spinal cord injury. *Journal of Neuropathology & Experimental Neurology* 75(1):69–85 DOI 10.1093/jnen/nlv002.
- Baazil H, Dalemans A, De Smet L, Degreef I. 2015.** Comparison of surgical treatments for mucous cysts of the distal interphalangeal joint. *Acta Orthopaedica Belgica* 81:213–217.
- Bertelli JA, Mira J-C. 1993.** Behavioral evaluating methods in the objective clinical assessment of motor function after experimental brachial plexus reconstruction in the rat. *Journal of Neuroscience Methods* 46(3):203–208 DOI 10.1016/0165-0270(93)90068-3.
- Birrell MT, Fuller A. 2019.** Twice daily cefazolin is effective for treatment of serious methicillin-sensitive *Staphylococcus aureus* infection in an outpatient parenteral antimicrobial therapy program. *Therapeutic Advances in Infectious Disease* 6:2049936119882847 DOI 10.1177/2049936119882847.
- Cao Y, Shumsky J, Sabol M, Kushner R, Strittmatter S, Hamers F, Lee D, Rabacchi S, Murray M. 2008.** Nogo-66 receptor antagonist peptide (NEP1-40) administration promotes functional recovery and axonal growth after lateral funiculus injury in the adult rat. *Neurorehabilitation and Neural Repair* 22(3):262–278 DOI 10.1177/1545968307308550.
- Carlstedt T. 2008.** Root repair review: basic science background and clinical outcome. *Restorative Neurology and Neuroscience* 26:225–241.
- Chen MS, Huber AB, van der Haar ME, Frank M, Schnell L, Spillmann AA, Christ F, Schwab ME. 2000.** Nogo-A is a myelin-associated neurite outgrowth inhibitor and an antigen for monoclonal antibody IN-1. *Nature* 403(6768):434–439 DOI 10.1038/35000219.

- Ci T, Chen L, Yu L, Ding J. 2014. Tumor regression achieved by encapsulating a moderately soluble drug into a polymeric thermogel. *Scientific Reports* 4(1):5473 DOI 10.1038/srep05473.
- Ciaramitaro P, Padua L, Devigili G, Rota E, Tamburin S, Eleopra R, Cruccu G, Truini A, Society NpsigotIN. 2017. Prevalence of neuropathic pain in patients with traumatic brachial plexus injury: a multicenter prospective hospital-based study. *Pain Medicine* 18(3):2428–2432 DOI 10.1093/pm/pnw360.
- Cullheim S, Carlstedt T, Risling M. 1999. Axon regeneration of spinal motoneurons following a lesion at the cord-ventral root interface. *Spinal Cord* 37(12):811–819 DOI 10.1038/sj.sc.3100916.
- Ding L, Zhu Z, Wang Y, Zeng L, Wang T, Luo J, Zou T-B, Li R, Sun X, Zhou G, Liu X, Wu H-F. 2019. LINGO-1 shRNA Loaded by Pluronic F-127 promotes functional recovery after ventral root avulsion. *Tissue Engineering Part A* 25(19–20):1381–1395 DOI 10.1089/ten.tea.2018.0282.
- Duijnsveld BJ, Henseler JF, Reijnierse M, Fiocco M, Kan HE, Nelissen RG. 2017. Quantitative Dixon MRI sequences to relate muscle atrophy and fatty degeneration with range of motion and muscle force in brachial plexus injury. *Magnetic Resonance Imaging* 36:98–104 DOI 10.1016/j.mri.2016.10.020.
- Eggers R, Tannemaat M, Ehlert E, Verhaagen J. 2010. A spatio-temporal analysis of motoneuron survival, axonal regeneration and neurotrophic factor expression after lumbar ventral root avulsion and implantation. *Experimental Neurology* 223(1):207–220 DOI 10.1016/j.expneurol.2009.07.021.
- Faglioni W, Siqueira MG, Martins RS, Heise CO, Foroni L. 2014. The epidemiology of adult traumatic brachial plexus lesions in a large metropolis. *Acta Neurochirurgica* 156(5):1025–1028 DOI 10.1007/s00701-013-1948-x.
- Gibon E, Romana C, Vialle R, Fitoussi F. 2016. Isolated C5-C6 avulsion in obstetric brachial plexus palsy treated by ipsilateral C7 neurotization to the upper trunk: outcomes at a mean follow-up of 9 years. *Journal of Hand Surgery* 41(2):185–190 DOI 10.1177/1753193415593493.
- GrandPré T, Li S, Strittmatter SM. 2002. Nogo-66 receptor antagonist peptide promotes axonal regeneration. *Nature* 417(6888):547–551 DOI 10.1038/417547a.
- Gu HY, Chai H, Zhang JY, Yao ZB, Zhou LH, Wong WM, Bruce I, Wu WT. 2004. Survival, regeneration and functional recovery of motoneurons in adult rats by reimplantation of ventral root following spinal root avulsion. *European Journal of Neuroscience* 19(8):2123–2131 DOI 10.1111/j.0953-816X.2004.03295.x.
- Huang C, Fu C, Qi ZP, Guo WL, You D, Li R, Zhu Z. 2020. Localised delivery of quercetin by thermo-sensitive PLGA-PEG-PLGA hydrogels for the treatment of brachial plexus avulsion. *Artificial Cells, Nanomedicine, and Biotechnology* 48(1):1010–1021 DOI 10.1080/21691401.2020.1770265.
- Kempf A, Schwab ME. 2013. Nogo-A represses anatomical and synaptic plasticity in the central nervous system. *Physiology* 28(3):151–163 DOI 10.1152/physiol.00052.2012.
- Kusaba T. 2009. Safety and efficacy of cefazolin sodium in the management of bacterial infection and in surgical prophylaxis. *Clinical Medicine Therapeutics* 1:1607–1615.
- Lang E, Schlegel N, Sendtner M, Asan E. 2005. Effects of root replantation and neurotrophic factor treatment on long-term motoneuron survival and axonal regeneration after C7 spinal root avulsion. *Experimental Neurology* 194(2):341–354 DOI 10.1016/j.expneurol.2005.02.018.
- Li S, Strittmatter SM. 2003. Delayed systemic Nogo-66 receptor antagonist promotes recovery from spinal cord injury. *Journal of Neuroscience* 23(10):4219–4227 DOI 10.1523/JNEUROSCI.23-10-04219.2003.

- Li H, Wong C, Li W, Ruven C, He L, Wu X, Lang BT, Silver J, Wu W. 2015. Enhanced regeneration and functional recovery after spinal root avulsion by manipulation of the proteoglycan receptor PTP σ . *Scientific Reports* 5(1):14923 DOI 10.1038/srep14923.
- Limthongthang R, Bachoura A, Songcharoen P, Osterman AL. 2013. Adult brachial plexus injury: evaluation and management. *Orthopedic Clinics* 44:591–603.
- Luo J, Borgens R, Shi R. 2004. Polyethylene glycol improves function and reduces oxidative stress in synaptosomal preparations following spinal cord injury. *Journal of Neurotrauma* 21(8):994–1007 DOI 10.1089/0897715041651097.
- Macaya D, Spector M. 2012. Injectable hydrogel materials for spinal cord regeneration: a review. *Biomedical Materials* 7(1):012001 DOI 10.1088/1748-6041/7/1/012001.
- Meng XL, Fu P, Wang L, Yang X, Hong G, Zhao X, Lao J. 2020. Increased EZH2 levels in anterior cingulate cortex microglia aggravate neuropathic pain by inhibiting autophagy following brachial plexus avulsion in rats. *Neuroscience Bulletin* 36(7):793–805 DOI 10.1007/s12264-020-00502-w.
- Meng C, Yang X, Liu Y, Zhou Y, Rui J, Li S, Xu C, Zhuang Y, Lao J, Zhao X. 2019. Decreased expression of lncRNA Malat1 in rat spinal cord contributes to neuropathic pain by increasing neuron excitability after brachial plexus avulsion. *Journal of Pain Research* 12:1297–1310 DOI 10.2147/JPR.
- Mingorance A, Solé M, Munetón V, Martínez A, Nieto-Sampedro M, Soriano E, del Río JA. 2006. Regeneration of lesioned entorhino-hippocampal axons in vitro by combined degradation of inhibitory proteoglycans and blockade of Nogo-66/NgR signaling. *The FASEB Journal* 20(3):491–493 DOI 10.1096/fj.05-5121fje.
- Nakamura Y, Fujita Y, Ueno M, Takai T, Yamashita T. 2011. Paired immunoglobulin-like receptor B knockout does not enhance axonal regeneration or locomotor recovery after spinal cord injury. *Journal of Biological Chemistry* 286(3):1876–1883 DOI 10.1074/jbc.M110.163493.
- National C, Promising I. 2009. *The National Academies Collection: reports funded by National Institutes of Health - NCBI Bookshelf*. Washington, D.C.: National Academies Press.
- Rong X, Ji Y, Zhu X, Yang J, Qian D, Mo X, Lu Y. 2019. Neuroprotective effect of insulin-loaded chitosan nanoparticles/PLGA-PEG-PLGA hydrogel on diabetic retinopathy in rats. *International Journal of Nanomedicine* 14:45 DOI 10.2147/IJN.
- Shin AY, Spinner RJ, Steinmann SP, Bishop AT. 2005. Adult traumatic brachial plexus injuries. *JAAOS-Journal of the American Academy of Orthopaedic Surgeons* 13(6):382–396 DOI 10.5435/00124635-200510000-00003.
- Shrestha B, Coykendall K, Li Y, Moon A, Priyadarshani P, Yao L. 2014. Repair of injured spinal cord using biomaterial scaffolds and stem cells. *Stem Cell Research & Therapy* 5(4):91 DOI 10.1186/scrt480.
- So K-F, Xu X-M. 2015. *Neural regeneration*. Cambridge: Academic Press.
- Soderblom C, Luo X, Blumenthal E, Bray E, Lyapichev K, Ramos J, Krishnan V, Lai-Hsu C, Park KK, Tsoulfas P. 2013. Perivascular fibroblasts form the fibrotic scar after contusive spinal cord injury. *Journal of Neuroscience* 33(34):13882–13887 DOI 10.1523/JNEUROSCI.2524-13.2013.
- Steward O, Sharp K, Yee KM, Hofstadter M. 2008. A re-assessment of the effects of a Nogo-66 receptor antagonist on regenerative growth of axons and locomotor recovery after spinal cord injury in mice. *Experimental Neurology* 209(2):446–468 DOI 10.1016/j.expneurol.2007.12.010.
- Teixeira MJ, da Paz MGds, Bina MT, Santos SN, Raicher I, Galhardoni R, Fernandes DT, Yeng LT, Baptista AF, De Andrade DC. 2015. Neuropathic pain after brachial plexus

avulsion-central and peripheral mechanisms. *BMC Neurology* **15**(1):73
DOI [10.1186/s12883-015-0329-x](https://doi.org/10.1186/s12883-015-0329-x).

- Wang Z, Fan J, Yang X, Zhang W, Zhang P, Jiang B. 2018.** The neural regeneration effect of chitin biological absorbable tubes bridging sciatic nerve defects with sural nerve grafts. *American Journal of Translational Research* **10**:2362.
- Wang F, Liang Z, Hou Q, Xing S, Ling L, He M, Pei Z, Zeng J. 2007.** Nogo-A is involved in secondary axonal degeneration of thalamus in hypertensive rats with focal cortical infarction. *Neuroscience Letters* **417**(3):255–260 DOI [10.1016/j.neulet.2007.02.080](https://doi.org/10.1016/j.neulet.2007.02.080).
- Xu J, He J, He H, Peng R, Xi J. 2017.** Comparison of RNAi NgR and NEP1-40 in acting on axonal regeneration after spinal cord injury in rat models. *Molecular Neurobiology* **54**(10):8321–8331 DOI [10.1007/s12035-016-0315-3](https://doi.org/10.1007/s12035-016-0315-3).
- Young W. 1996.** Spinal cord regeneration. *Science* **273**:451.
- Zhai ZY, Feng J. 2019.** Constraint-induced movement therapy enhances angiogenesis and neurogenesis after cerebral ischemia/reperfusion. *Neural Regeneration Research* **14**(10):1743–1754 DOI [10.4103/1673-5374.257528](https://doi.org/10.4103/1673-5374.257528).
- Zhang Z, Ni J, Chen L, Yu L, Xu J, Ding J. 2011.** Biodegradable and thermoreversible PCLA-PEG-PCLA hydrogel as a barrier for prevention of post-operative adhesion. *Biomaterials* **32**(21):4725–4736 DOI [10.1016/j.biomaterials.2011.03.046](https://doi.org/10.1016/j.biomaterials.2011.03.046).
- Zhang K, Tang X, Zhang J, Lu W, Lin X, Zhang Y, Tian B, Yang H, He H. 2014.** PEG-PLGA copolymers: their structure and structure-influenced drug delivery applications. *Journal of Controlled Release* **183**:77–86 DOI [10.1016/j.jconrel.2014.03.026](https://doi.org/10.1016/j.jconrel.2014.03.026).
- Zhao J, Guo B, Ma PX. 2014.** Injectable alginate microsphere/PLGA-PEG-PLGA composite hydrogels for sustained drug release. *RSC Advances* **4**(34):17736–17742 DOI [10.1039/c4ra00788c](https://doi.org/10.1039/c4ra00788c).
- Zhou Y, Liu P, Rui J, Zhao X, Lao J. 2017.** The associated factors and clinical features of neuropathic pain after brachial plexus injuries. *The Clinical Journal of Pain* **33**(11):1030–1036 DOI [10.1097/AJP.0000000000000493](https://doi.org/10.1097/AJP.0000000000000493).